JOURNAL OF GEOPHYSICAL RESEARCH, VOL. 86, NO. C9, PAGES 8085–8092, SEPTEMBER 20, 1981

Bubble and Aerosol Spectra Produced by a Laboratory 'Breaking Wave'

RAMON J. CIPRIANO AND DUNCAN C. BLANCHARD

Atmospheric Sciences Research Center, State University of New York at Albany, Albany, New York 12222

The relative contribution of jet and film drops from bursting bubbles to the sea-salt component of the marine aerosol is poorly understood. An analysis of the bubble and aerosol spectra produced by a laboratory model of a breaking wave or whitecap shows that film drops may play a much more important role than previously accorded. The model strongly suggests that most of the droplets smaller than 5–10 μm in diameter originate as film drops, derived from bubbles larger than 1 mm. The water-to-air flux of such droplets is adequate to account for the majority of maritime cloud condensation nuclei. The model also suggests that droplets larger than 20–25 μm originate as jet drops, derived from bubbles smaller than 1 mm. The model breaking wave produces an upwelling plume of bubbles whose concentration for all bubble sizes vastly exceeds the steady state or background bubble population observed at sea at depths greater than 1 m. Bubbles of up to 10 mm diameter were produced, and the bubble flux reached 200 cm^{-2} s^{-1}. Whitecap bubble spectra, presently unavailable, are therefore essential in making more accurate assessments of marine aerosol production.

INTRODUCTION

A major source of the sea-salt component of the marine aerosol is the bursting of whitecap-produced bubbles [*Blanchard and Woodcock,* 1980]. Bursting bubbles produce two types of droplets: film drops, from the rupture of the bubble film, and jet drops, by the breakup of the vertically rising jet of water from the collapsing bubble cavity [*Blanchard,* 1975]. Jet drops are of the order of one tenth the bubble diameter [*Blanchard and Woodcock,* 1957]. The number of jet drops per bubble decreases from as many as five or six for a 300 μm diameter bubble to only one for bubbles larger than about 3 mm. Conversely, the number of film drops per bubble increases with increasing bubble diameter: bubbles smaller than ~300 μm produce no film drops, a 2 mm bubble produces up to 100, and a 6 mm bubble up to 1000 [*Blanchard,* 1963; *Day,* 1963]. Film-drop size distributions have been obtained by *Blanchard and Syzdek* [1975], M. Tomaides and K. T. Whitby (unpublished data, 1975), and *Cipriano* [1979], although the data are not as complete as those for jet drops.

It is clear from the above that the relative contribution of jet and film drops to aerosol production depends critically on the shape of the bubble spectrum. *Moore and Mason* [1954] noted that if the majority of bubbles produced by breaking waves are larger than about 500 μm, relative jet drop contribution would be minimal, since the terminal velocity of jet drops from such larger bubbles prevents their remaining airborne. Partially on the basis of their laboratory simulation of wave breaking, they suggest that airborne salt nuclei $< 10^{-9}$ g (i.e., seawater drops < 40 μm diameter) originate as film drops. *Blanchard and Woodcock* [1957] measured the bubble spectrum near a small whitecap and found the population of bubbles <500 μm to be far greater than those larger, implying a jet drop mode of origin. However, *Blanchard* [1963] and *Blanchard and Woodcock* [1980] note that estimates of the relative contribution of the two types of droplets, which are based on their observed whitecap bubble spectrum, must be regarded with caution, since experimental difficulties prevented the measurement of bubbles >500 μm.

The experiments discussed here were undertaken as a first step in addressing this problem. The main approach was to make observations of both bubble and aerosol spectra produced by a laboratory simulation of a breaking wave. The observed bubble spectra, in conjunction with extant laboratory data on the numbers and sizes of jet and film drops produced by individually bursting bubbles, can be used to calculate the resultant aerosol spectrum. The estimated spectrum can then be compared to that actually observed.

How does one produce a bubble spectrum? Many investigators (including the authors) have attempted to simulate the vigorous splashing and bubbling that occurs when a wave breaks at sea by forcing air through a glass frit or sparger immersed in seawater. However, the bubble spectrum depends on frit pore size and airflow rate and is thus rather arbitrary. In nature, the whitecap bubble spectrum results from the breakup of large volumes of air entrained by the breaking wave. We believe this process is analogous to what occurs when falling water breaks up to produce a raindrop spectrum: above a certain rain intensity, the shape of the raindrop spectrum remains constant, although the total number of drops continues to increase [*Blanchard and Spencer,* 1970; *Srivastava,* 1978]. In like manner, it is not unreasonable to expect that as the volume of entrained air increases, its breakup produces bubble spectra that approach a characteristic shape. Therefore, we believe that in the laboratory we can model a bubble spectrum whose shape approaches that produced by whitecaps at sea. Thus, we should be able to get meaningful data on the relative importance of large and small bubbles and of jet and film drops.

EXPERIMENTAL PROCEDURE

Figure 1 shows the basic experimental arrangement. It consisted of a small tank, a centrifugal pump, and a wier-like device. The tank was filled with seawater at 26° ± 2°C. The pump was used to fill the wier, which, perched about 33 cm above the water surface, produced a continuous waterfall. This falling water (~410 cm^3 s^{-1}) entrained air in a manner similar to a type of wave known as a plunging breaker, found in both shallow and deep water [*Cokelet,* 1977]. The entrained air produced a plume of bubbles that rose to the surface,

Paper number 1C0713.
0148-0227/81/001C-0713$01.00

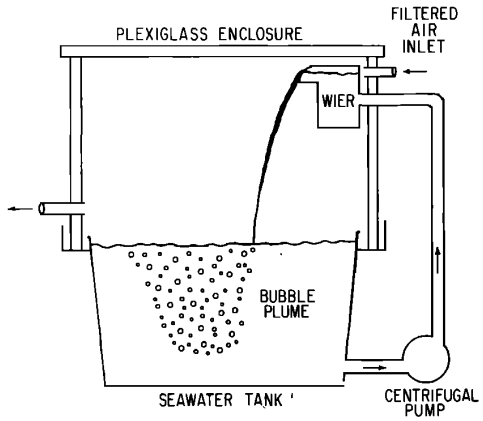

Fig. 1. Simplified scale drawing of model breaking wave. Seawater tank is 0.5 m in diameter at top, 26.5 cm deep.

burst, and ejected an aerosol that was confined by the Plexiglas enclosure.

The bubble spectra were measured photographically, with the aid of two 'bubble collectors' shown schematically in Figure 2*a*. These each consisted of two parallel glass plates, sealed at the top and sides. The bottom of a collector was submerged 1–2 cm in the region of the tank surface to be examined. Then, by controlling the pressure drop inside the collector with a vacuum pump, a slab of bubble-containing water could be drawn up to nearly the top and held in position indefinitely. Since the distance between the plates (A) was small

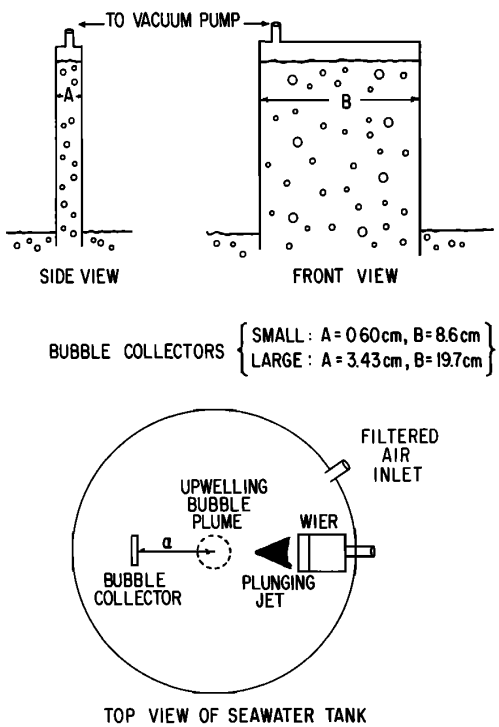

Fig. 2. Bubble collectors used for the photographic determination of bubble spectra, and view of seawater tank surface. The parameter α denotes the distance between the center of the upwelling plume of bubbles and the collector.

compared to the field of view (B), the bubbles were confined to the focal plane of the camera (Rollei SL66), eliminating depth-of-field error. Two collectors were necessary to cover the broad range of bubble sizes encountered (~50 μm to ~8 mm diameter). The spectrum of bubbles reaching the tank surface of course depends on how close to the center of the upwelling bubble plume the collector is placed. Calling this distance α (Figure 2*b*), photographs were taken at α = 0, 2, 7, and 12 cm. Approximately 6×10^3 bubbles were thus counted and classed by size.

It must be emphasized that this laboratory simulation avoids a number of difficulties inherent in measuring the whitecap bubble production rate at sea, not the least of which relates to sampling time. When a wave breaks, the largest bubbles surface first, and thus the bubble spectrum is a function of time as well as position in the whitecap. To obtain the total number of bubbles produced, a sequence of spectra in both space and time must be secured, an extremely difficult if not impossible task. In the present case, the time dependence is eliminated by operating the system in a steady state. The bubble population at a given position in the upwelling plume is constant; bubbles rise continuously through the collectors and can be photographed at leisure.

To obtain the aerosol spectra, filtered air was passed into the Plexiglas enclosure at a rate F_a. This airstream served to mix with and dilute the aerosol within. By varying F_a (i.e., mean particle residence time in the enclosure) the sedimentation loss could be evaluated. Relative humidity (RH) was monitored with an Assman psychrometer. The large end of the aerosol spectrum was measured with a Royco® model 225 optical particle counter (particle diameter from 0.5 to 15 μm, in five channels). Gardner counters were used to measure condensation nuclei (CN) concentrations. Although the count was too low to obtain size discrimination of the submicron portion with an electrical aerosol analyzer [*Liu and Pui*, 1975], some useful results were obtained with a Sinclair diffusion battery [*Sinclair et al.*, 1976]. Particle loss by diffusion and impaction was taken into consideration.

Further details on experimental technique are discussed at length elsewhere [*Cipriano*, 1979].

RESULTS

Bubble Spectra

Bubble histograms for α = 0 and α = 7 cm are shown in Figure 3. The spectra are very similar up to bubble diameters of about 1 mm; these smaller bubbles are more easily dispersed horizontally owing to their slower rise speeds. As bubble size increases from 1 to 10 mm, the population at α = 7 cm falls increasingly short of that at α = 0 cm, the plume center. However, the most important thing to note here is the rather substantial number of bubbles larger than 1 mm, in either case. For example, at α = 0, the number in the 100–300 μm interval is only about 2 orders of magnitude greater than those in the 4–5.6 mm interval, and about 1 order of magnitude greater than those in the 2–2.8 mm interval. Recalling that each 2-mm bubble may produce ~100 film drops, that each 100–300 μm bubble can produce ~5 jet drops, and allowing for the fact that the larger bubbles have about a 5 fold greater rise speed, one notes that film drop production may be 10 times as efficient as that of jet drops in this simple example.

The spectrum at α = 12 cm, nearly at the tank edge, is shown in Figure 4 (solid line). Smaller bandwidths have been

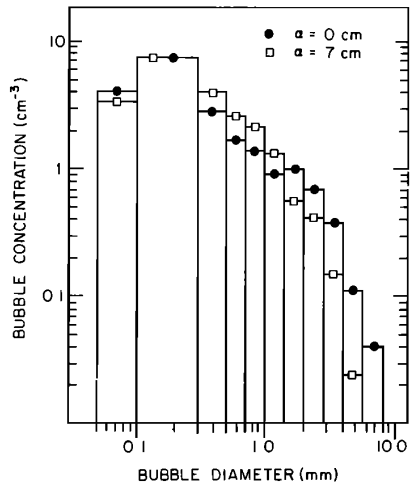

Fig. 3. Bubble frequency distributions for $\alpha = 0$ and 7 cm. Size thresholds are 0.05, 0.1, 0.3, 0.5, 0.7, 1.0, 1.4, 2.0, 2.8, 4.0, 5.6, and 8.0 mm.

used to provide greater resolution. Bubbles larger than 1 mm are almost completely absent here, whereas the number between 100 and 300 μm (~4 + 2.3 = 6.3/cm^3) is nearly the same as at $\alpha = 0$ or 7 cm (~7.2/cm^3). This again reflects the rapid depletion of larger bubbles with increasing distance from the center of the upwelling bubble plume, in contrast to the rather uniform dispersion of the smaller bubbles.

Three observed oceanic spectra, reduced to equivalent bandwidth, are also presented in Figure 4. *Blanchard and Woodcock* [1957] obtained their data (dashed line) at a depth of about 10 cm, a few seconds after a breaking wave had passed. They had to wait several seconds to allow the largest bubbles (several millimeters) to rise first to the surface, to avoid bubble interference in their collector (a Plexiglas box). Their spectrum agrees well with that of the model wave for the smallest size interval (100–200 μm), but shows increasingly fewer bubbles as size increases to 1 mm. This is easily attributable to the delay before sampling. In 3 s, bubbles of 600 μm diameter rise about 24 cm. Thus, if any 600-μm bubbles are sampled, they must be those from the portion of the whitecap-produced plume that extends below 24 cm. This is substantial distance, since the penetration depth of the bubble plume is of the order of the waterfall height (Figure 1).

The results of *Johnson and Cooke* [1979] and *Kolovayev* [1976], who employed photographic techniques, are also shown in Figure 4, at depths of 0.7 m (sawtooth) and 1.5 m (dot-dash), respectively. Their data represent a steady state or background bubble spectrum, since no specific attempt was made to sample in a region immediately after a wave had broken. Comparison of all spectra in Figure 4 shows clearly that the population of larger bubbles becomes increasingly depleted as sampling depth increases and as the time elapsed between bubble production and sampling increases. Even at a depth of only 70 cm, few bubbles larger than about 400 μm diameter are observed.

Bubble and Aerosol Production Rates

A comparison between estimated and observed droplet production via bursting bubbles requires a knowledge of the total bubble production rate of the model wave. This is the same as the number of bubbles reaching the surface of the tank per unit time (in given size intervals), since the production rate in the steady state must equal the rate at which they arrive at the surface and burst. The bubble production rate per unit area (bubble flux) is simply equal to the product of bubble concentration and rise speed. The bubble flux is a function of α and when integrated over the whole tank surface gives the bubble production rate.

The result of this integration is shown in Figure 5. Note that the relative production of bubbles in the 1.0–1.4 mm interval versus the 100–300 ~μm interval is actually greater than the relative concentration of bubbles in these two classes near the plume center (Figure 4). In other words, total bubble production falls off less rapidly with increasing size than bubble concentration, even at $\alpha = 0$ where the large bubble population is a maximum. This is because the much greater rise speed of the larger bubbles more than compensates for their more limited horizontal dispersion.

The data in Figure 5 can be viewed as a reasonable first approximation of the relative numbers of bubbles of various sizes produced by the breakup of entrained air in seawater at 26°C. The total rate of air entrainment can be found either by direct measurement (i.e., by capturing the air contributed by all the bursting bubbles) or by calculation from Figure 5. Both methods gave a value of 125 ± 17 cm^3 s^{-1}, nearly a third of the volume flow of water, illustrating the efficiency with which air is entrained by falling water. Less than 5% of the entrained air is converted into bubbles smaller than 1 mm in diameter.

The aerosol production rate is similarly defined as the total number of droplets of various sizes produced by the model wave per unit time. The production rate of droplets sampled by the Royco counter is shown in Figure 6, reduced to show original or unevaporated droplet diameter (for seawater, the diameter of the salt nucleus, assuming sphericity, is approximately one fourth the unevaporated drop diameter). The error

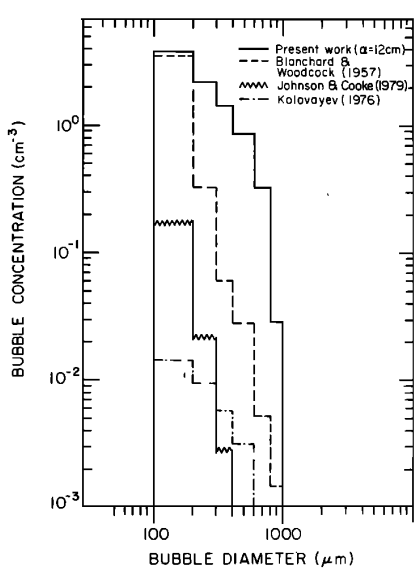

Fig. 4. Bubble frequency distributions of model wave (solid line) compared with those observed at sea: dashed line, depth 10 cm, light winds; sawtooth line, depth 70 cm, winds 20–25 kn; dot-dash line, depth 150 cm, winds 22–26 kn. Size thresholds are 100, 200, 300, 400, 600, 800, and 1000 μ.

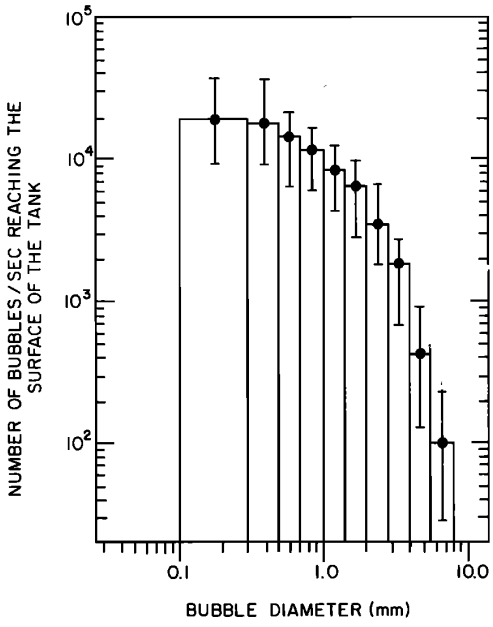

Fig. 5. Steady state total bubble production rate (frequency distribution) of the model breaking wave.

bars increase toward the largest drop sizes owing to the increasing difficulty in evaluating sedimentation loss. When summed over the five channels, the production rate is 1.4×10^5 s^{-1} (± 25%). The condensation nuclei production rate was found to be 2.7×10^5 s^{-1} (± 15%), from which we infer that approximately half the droplets are of submicron size. Measurements with the diffusion battery showed the presence of particles as small as 0.03 μm diameter, at RH = 90%, or 0.014 μm diameter as dry sea salt. This suggests the bubble bursting process can directly produce very small particles, without invoking a shattering mechanism via phase change [*Iribarne et al.*, 1977].

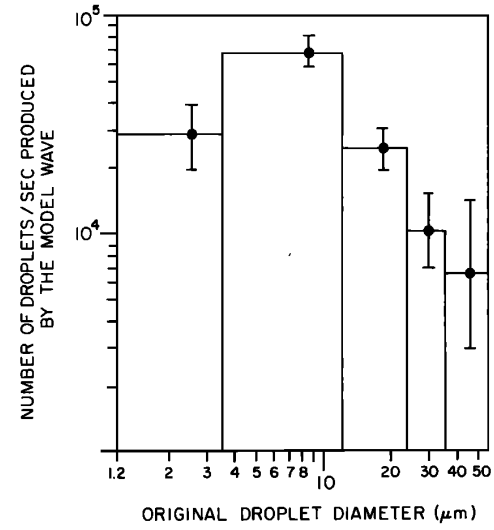

Fig. 6. Observed model wave droplet production, for diameter >1 μm. Size thresholds are 1.2, 3.5, 12, 36, and 56 μm.

Comparison of Bubble and Aerosol Production

To obtain an estimate of the total jet-drop production rate we need only combine the observed bubble production rate (Figure 5) with the empirical relationship between bubble diameter and jet-drop diameter [*Blanchard and Woodcock*, 1957]. The result is shown in Figure 7, assuming an average of five jet drops per bubble. The upper and lower bounds for each size interval correspond to the upper and lower bounds of the bubble production rate; these in turn resulted from the integration process used to sum over the tank surface, which was partitioned into a finite number of regions (i.e., the four corresponding to the values of α at which bubble spectra were measured).

Comparison of Figure 7 with the observed droplet production (Figure 6) reveals that the estimated jet-drop production rate is certainly adequate to explain the production of droplets with a diameter > 20 μm. Of course, most of the very large droplets (> 100 μm) are unable to remain airborne and fall back into the water. For drops in the smallest interval seen by the Royco (i.e., 1.2 to 3.5 μm unevaporated diameter), Figure 6 suggests a bubble production rate of around $(3 \times 10^4)/5 = 6 \times 10^3$ s^{-1} (again assuming five jet drops/bubble), whose diameter must be between about 12 and 35 μm. Although bubbles of this size were beyond the resolution of the camera lens, their presence in sufficient number is highly questionable. Bubbles this small are forced back into solution soon after they are formed [*Blanchard and Woodcock*, 1957; *Johnson and Cooke*, 1979], owing to their high internal pressure. The observed bubble spectra (Figure 3) suggest that a maximum in the distribution is occuring somewhere between 100 and 300 μm. *Johnson and Cooke* [1979] and *Kolovayev* [1976] were capable of resolving bubbles of 35 μm diameter. Both found a definite peak in the size distribution, at 100–150 μm, with concentration falling off sharply with decreasing bubble diameter. In the sea the absence of these smaller bubbles cannot be attributed to the fact that the samples were not obtained at the surface directly in a whitecap, for their rise speed (<0.5 cm/s) is small compared with eddies and currents in the water. Such

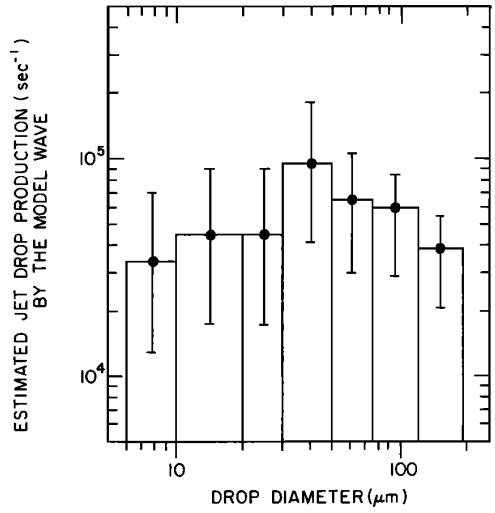

Fig. 7. Calculated jet-drop production derived from observed model wave bubble production, assuming five drops per bubble. Totals for all intervals: upper bound, 7.0×10^5 s^{-1}; best estimate, 3.9×10^5 s^{-1}; lower bound, 1.7×10^5 s^{-1}.

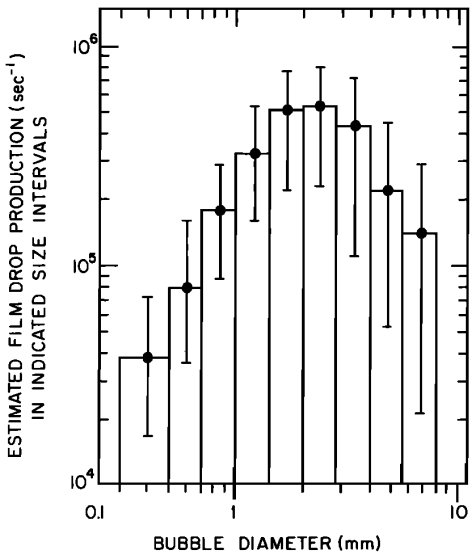

Fig. 8. Calculated film-drop production derived from observed model wave bubble production, using the upper bound data of *Blanchard* [1963] and *Day* [1963]. Totals for all intervals: upper bound, 4.0 × 10^6 s^{-1}; best estimate, 2.5 × 10^6 s^{-1}; lower bound, 1.0 × 10^6 s^{-1}.

currents would surely be able to disperse these bubbles to a depth of 70 cm.

Oceanic bubble spectra obtained by *Medwin* [1977] and *Lovik* [1980] from acoustic methods do not display a relative maximum over the range measured: bubble diameters from 20 to 630 μm. *Wu* [1981] has compared Medwin's spectra with those of Johnson and Cooke and Kolovayev. For bubble diameter >120 μm, all have similar shapes. Wu concludes that bubbles <120 μm diameter observed by Medwin must have been produced by mechanisms other than air entrainment at the surface, particularly since their concentration does not decrease with depth.

The number of film drops produced by a bursting bubble is highly variable, being greatly affected by the presence of organic surface films on the water surface [*Blanchard,* 1963; *Day* 1963; *Paterson and Spillane,* 1969]. If such films were not present, and if the bubbles were to burst immediately upon arrival at the surface then large bubbles produce the number of film drops previously mentioned; even if they do not burst immediately, they sometimes produce the maximum number of film drops [*Blanchard,* 1963]. In these experiments, the great flux of bubbles near the plume center created an upwelling that was more than adequate to prevent the buildup of surfactants [*Blanchard and Syzdek,* 1974]. Measurements of bubble rise speed (via streak photography) showed that the larger bubbles were rising as fluid rather than as rigid spheres, which in turn suggests [*Detwiler and Blanchard,* 1978] that they did not adsorb a surfactant coating while rising to the surface; this could conceivably have the same suppressive effect on film-drop production as a surfactant coating on the bulk water surface. Therefore, the upper bound film-drop production observed by *Blanchard* [1963] and *Day* [1963] for immediately bursting bubbles is used to calculate film drop production. (Jet drop production is also suppressed by a surfactant coating, although to a some what lesser extent.)

The film-drop production rate calculated from the observed bubble production rate is shown in Figure 8. Since the relationship between bubble diameter and film-drop size distribution is unknown except for a few specific cases, bubble diameter (rather than drop diameter) appears on the abscissa. The size intervals are the same as those in Figures 3 and 5; upper and lower bounds were derived as in Figure 7.

Casual comparison of Figures 7 and 8 shows that the calculations yield far more film drops than jet drops; the ratio of the best-estimate production rates is 2.5 × 10^6/3.9 × 10^5 = 6.4. This is in marked contrast to the *Blanchard and Woodcock* [1980] estimate of 1/75, based on their observed [*Blanchard and Woodcock,* 1957] bubble spectrum. However, as they noted, this spectrum is deficient in the population of larger bubbles.

Since about half of the droplets produced by the model wave were of submicron size, it is difficult to escape the conclusion that these originated as film drops, for otherwise we would have to assume the existence of numerous bubbles of diameter less than 10 μm, which can reach the surface and burst. Since the time required for a 10-μm bubble to be forced back into solution is less than 10 s, even for water that is 15% supersaturated with air [*Blanchard and Woodcock,* 1957], and since such bubbles have negligible rise speed, this scenario seems unlikely.

Figure 8 shows that estimated film-drop production reaches a maximum for bubbles of roughly 2 mm diameter; bubbles smaller than 1 mm or larger than 5 mm are relatively inefficient. Conversely, jet drop production falls off rapidly as bubble diameter increases beyond 1 mm. Even if it did not, these jet drops would have little effect, as they would remain airborne for only a few seconds at most.

Although film-drop size distributions are presently available only for selected bubble sizes, the data are sufficient to show that not only submicron drops, but also drops of up to perhaps 10 μm diameter, can be accounted for more easily via the film drop mechanism. For example, the bursting of 4.5-mm diameter bubbles in seawater was found [*Cipriano,* 1979] to produce an average of 170 film drops per bubble of 2–6 μm diameter. The production rate of bubbles in the 4–5.6 mm interval is 10^2 to 10^3 s^{-1} (Figure 5), which implies a 2–6 μm film-drop production rate of ~2 × 10^4 to 2 × 10^5 s^{-1}. To account for this via jet drops implies a production of at least 4 × 10^3 to 4 × 10^4 bubbles s^{-1} of 20–60 μm diameter (assuming 5 drops/bubble); for reasons already discussed the production of such bubbles at this rate is very doubtful. Note that in this comparison the calculated film-drop production from only one bubble-size interval has been used, and in particular one which is relatively inefficient; a fair comparison requires integration over all bubble size intervals. *Blanchard and Syzdek* [1975] and M. Tomaides and K. T. Whitby (unpublished data, 1975) found that most of the film drops they observed from a 1.4-mm bubble, which is close to the size for maximum production efficiency (Figure 8), were 1–10 μm in diameter.

Further evidence shedding light on the origin of the 1–10 μm drops was obtained in experiments in which the seawater was inoculated with a known concentration of bacteria. The aerosol thus produced was sampled with an Andersen cascade impactor [*Andersen,* 1958]. Droplets of 3–10 μm were found to be highly enriched in the bacteria. On the other hand, a number of laboratory experiments with single bubbles suggest that, although bacteria are enriched in jet drops of 30–60 μm diameter, little or no enrichment occurs for jet drops smaller than about 20 μm [*Blanchard,* 1978]. Finally, *Blanchard* [1963] and *Day* [1963] have shown that large (several millimeter)

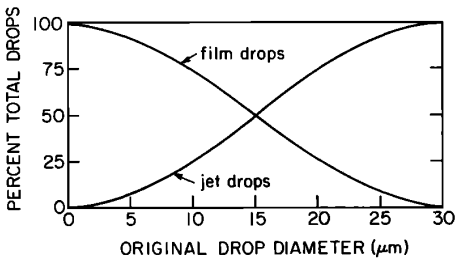

Fig. 9. Relative jet and film drop contribution inferred from analysis of the model wave. Diagram is a first approximation only and should not be interpreted in an exact sense.

bubbles eject most of their film drops to a height of several centimeters, whereas jet drops of diameter <6 μm are ejected to <0.3 cm height [*Blanchard,* 1963]; thus the film drops have a higher probability of remaining airborne.

Although the jet drop mechanism was adequate to explain the production of droplets >20 μm diameter, completeness requires consideration of film drops. The experiments with the 4.5-mm bubble showed that only one or two film drops per bubble were produced of 20–40 μm diameter. The production rate for this size bubble by the model wave is less than 10^3 (Figure 5) and yet the observed 20–40 μm droplet production rate is closer to 10^4 (Figure 6). Although more film drop data are required to give a definite answer, it seems unlikely that integration over all bubble size intervals can make up the difference, particularly since the 'more efficient' 1.4-mm bubbles produced hardly any droplets this large. But to produce 10^4 jet drops s^{-1} of 20–40 μm diameter requires only ~10^4 bubbles s^{-1} of 200–400 μm diameter, even allowing only one jet drop per bubble. Figure 5 shows that this is easily met.

For droplets of 'intermediate' diameter (i.e., 10-20 μm) there is apparently a region of overlapping contribution, in which as droplet size increases the film-drop influence fades away and jet-drop influence becomes dominant. This is shown semiqualitatively in Figure 9. *Woodcock* [1972], from an analysis of Hawaiian and Alaskan marine aerosols, suggested that a transition from jet to film drops occurs at 1 or 2 μm droplet diameter.

It should be noted that the best estimate of total film-drop production (2.5×10^6 s^{-1}) is about an order of magnitude greater than the observed total particle-production rate, for reasons that can only be speculated upon. Certainly, there are many complex events occurring in this mass-bubbling situation. At the center of the upwelling plume, large bubble flux is very great, and interference effects may be important. The water surface is not quiescent (as in single bubble experiments), but extremely agitated, which must surely affect the bursting process. In the lowest few centimeters above the water surface, droplet coalescence may occur. Around the periphery of the region of strong upwelling, a fraction of the largest bubbles do not burst immediately. While floating on the surface, some coalesce into giant (several centimeters) hemispheres while others cling together in rafts, as is observed at sea near breaking waves. This coalescence greatly reduces the bubble film area available for drop formation. Of course smaller bubbles, potential sources of both jet and film drops, continue to rise beneath these structures, which sometimes occupied a significant fraction of the water surface surrounding the region of strong upwelling. These bubbles might have been inhibited from bursting freely, suppressing drop production; even if not so inhibited, any droplets produced may have impacted onto the interiors of the floating bubbles.

These considerations illustrate the danger of making a simple linear extrapolation from the results of single-bubble experiments to the mass-bubbling situation. This precaution applies to both jet and film drops, particularly the latter. It must be reemphasized that the upper bound film drop production observed by *Blanchard* [1963] has been used, which for reasons such as the above may be inappropriate. Even in a situation where bubbles burst individually, all of the factors controlling film drop production are not understood. Therefore, the results of such extrapolation must be interpreted with caution. Nevertheless, the calculated ratio of film- to jet-drop production is striking. If the upper bound film drop versus bubble diameter relationship is reduced to one sixth, and the five jet drop per bubble assumption is left intact, one is still left with an equal contribution of both types of drops.

DISCUSSION

There are a number of difficulties inherent in comparing aerosol production by the model wave to that due to whitecaps at sea. Nevertheless, such a comparison is illuminating and has some interesting implications.

Consider first the production of condensation nuclei. From a knowledge of the background concentration of oceanic CN in regions remote from the continents, their residence time in the atmosphere, and the height through which they are distributed, one can calculate the sea-to-air flux required to maintain this steady state. *Blanchard* [1969] found this to be about 100 cm^{-2} s^{-1} for a background concentration of 200 cm^{-3}. *Mason* [1957] arrived at a similar result, though from a somewhat different line of reasoning.

Using this average value of 100 CN cm^{-2} s^{-1}, one can then calculate the flux that must exist over whitecaps. This requires a knowledge of the percentage of the sea normally covered with whitecaps. The estimation of the latter is compounded by the difficulty in formulating a precise definition of a whitecap. The most obvious definition, the area of water that appears white, is somewhat ambiguous, for the whiteness can be caused by foam patches and streaks, as well as regions of vigorously bubbling water [*Blanchard,* 1971]. Thus, data on oceanic whitecap coverage versus windspeed assembled from a number of workers show considerable scatter [*Monahan,* 1979]. *Blanchard* [1971] points out that areas of active bubbling may actually be underestimated in photographic studies of whitecap coverage. All things considered, with average wind conditions at sea a reasonable estimate of the percentage of the sea surface covered by areas where active bubbling (defined as an area where the flux of upwelling bubbles is sufficient to whiten the water) is taking place is ~3%. Using this, *Blanchard* [1969] calculated that the sea-to-air CN flux over the whitecaps was about 3×10^3 cm^{-2} s^{-1}.This compared favorably with the value of about 4000 cm^{-2} s^{-1} he deduced from CN measurements made both directly behind and away from regions where waves were breaking.

Can a CN flux of this order be produced by the model wave? The total (i.e., CN) droplet production of the model wave was ~3×10^5 s^{-1}. Visual inspection of the model showed that the diameter of the whitish region due to the upwelling bubble plume was no greater than about 16 cm. Within this region, droplet production is almost certainly dominated by the film-rupture mechanism. For example, Figure 10 shows

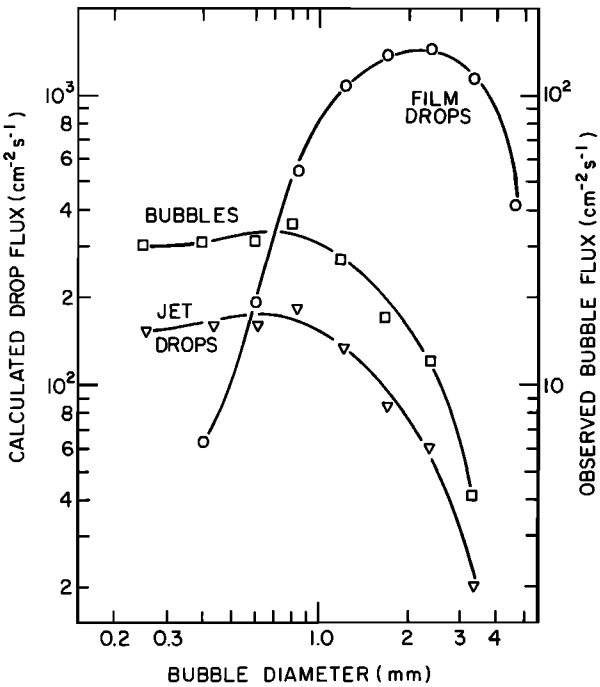

Fig. 10. Calculated jet and film drop flux produced by the bursting of the bubble spectrum observed at $\alpha = 7$ cm. Data points correspond to the size intervals of Figures 3, 5, or 8. Totals for all intervals: jet drops, 9.5×10^2 cm^{-2} s^{-1}; film drops, 6.2×10^3 cm^{-2} s^{-1}; bubbles, 1.9×10^2 cm^{-2} s^{-1}.

the flux of jet drops (allowing five per bubble) and film drops (the number per bubble according to *Blanchard* [1963] and *Day* [1963]) which could 'theoretically' be produced by the bursting of the bubble spectrum observed at $\alpha = 7$ cm. The bubble flux is also shown. Note that the observed flux of bubbles in the 1.0–1.4 mm interval is nearly as great as that for the 300–500 μm interval (i.e., their greater rise speed just compensates for their lower volume concentration). Figure 10 clearly shows the greater potential efficiency of the film-drop mechanism, even at $\alpha = 7$ cm near the 'edge' of the whitecap: The ratio of estimated film-to-jet drop production summed over all bubble size intervals is $6.2 \times 10^3/9.5 \times 10^2 = 6.6$, which is about the same as the relative production over the entire tank surface. (At $\alpha = 0$, this ratio is ~ 13!) Since the production of droplets of diameter <10 μm (assumed to be film drops) was $\sim 2.3 \times 10^5$ s^{-1} (the sum of the sub-micron fraction (1.3×10^5) and the smallest two size intervals in Figure 6) the average water-to-air flux of such droplets over the model whitecap is probably $\sim 10^3$ cm^{-2} s^{-1}. This is comparable to the values obtained above by *Blanchard* [1969] and is adequate to account for a third of the observed oceanic background CN count and probably all of the cloud condensation nuclei [*Mason*, 1971], bearing in mind the necessarily rough nature of such a calculation.

The water-to-air salt mass flux from the model wave is dominated by the largest drops, as should be apparent from Figure 6. Figure 11 shows this flux, averaged over the tank surface, where each data point represents the contribution from droplets in size intervals corresponding to those in Figure 6. Since at least 70% of the flux is due to droplets larger than ~23 μm, the model wave salt mass flux probably derives mostly from jet drops. The salt mass loading close to the sea surface can be shown [*Cipriano*, 1979] to be of the same order of magnitude as that over the model wave, again assuming 3% whitecap coverage. Thus, the model wave experiments suggest that most of the oceanic salt mass flux derives from jet drops. *Blanchard and Woodcock* [1980] have dubbed the lowest meter of the marine atmosphere the 'layer of influence of large jet drops.'

Blanchard and Hoffman [1978] have shown that the ejection height of jet drops is influenced by the adsorption of dissolved organic material onto the rising bubble. The effect is most pronounced on the larger bubbles (about 1 mm diameter). They note that this may not necessarily imply that organics in the sea play a role in modifying the drop-size spectrum produced by the sea, since most of the bubbles that produce jet drops are most likely smaller than 1 mm. If most of the drops larger than ~20 μm are jet drops, as the model suggests, the implication is that the salt mass loading the marine aerosol is unaffected by dissolved organics. However, evidence [*Blanchard*, 1963; *Day*, 1963; *Paterson and Spillane*, 1969] suggests that such organic adsorption may have a marked effect on film-drop production. If most of the drops smaller than ~10 μm are film drops, again as suggested by the model, then the presence of dissolved organics may exert a strong influence on the abundance of such droplets as well as on their composition.

The geochemical fractionation exhibited by the marine aerosol generally increases with decreasing particle size. If the small end of the marine aerosol spectrum is indeed dominated by film drops, an estimation of this fractionation based on oceanic bubble spectra may require a knowledge of the spectra in the immediate vicinity of breaking waves. Such information is presently unavailable. Particular attention should be paid to the larger bubbles, since their number decreases rapidly with distance from the whitecap. If whitecap bubble spectra can be obtained, they could probably be reproduced

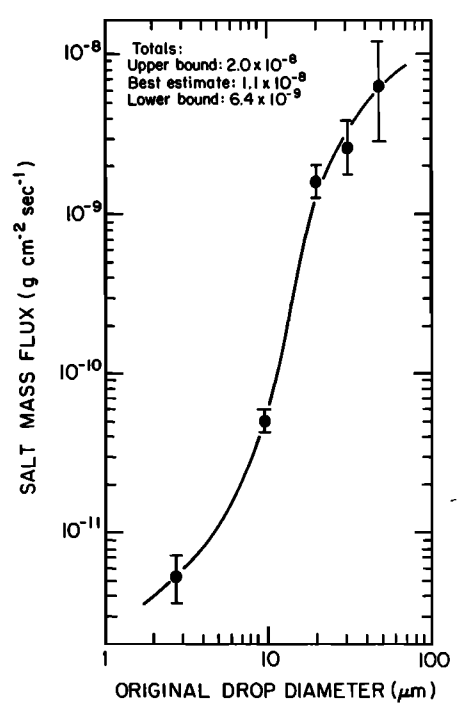

Fig. 11. Observed water-to-air salt mass flux produced by the model wave, averaged over the tank surface. Drop size intervals correspond to Figure 6.

artificially. This would enable more realistic simulations of the fractionation process, both in the laboratory and at sea.

Acknowledgment. The support of this work by the National Science Foundation under grant ATM78-00782 and ATM7912144 is gratefully acknowledged.

REFERENCES

Andersen, A. A., New sampler for the collection, sizing and enumeration of viable airborne particles, J. Bacteriol., *76,* 471–484, 1958.

Blanchard, D. C., The electrification of the atmosphere by particles from bubbles in the sea, *Prog. Oceanogr., 1,* 71–202, 1963.

Blanchard, D. C., The oceanic production rate of cloud nuclei, *J. Rech. Atmos., 4,* 1–6, 1969.

Blanchard, D. C., Whitecaps at sea, *J. Atmos. Sci., 28,* 645, 1971.

Blanchard, D. C., Bubble scavenging and the water-to-air transfer of organic material in the sea, in Applied Chemistry at Protein Interfaces, *Advan. in Chem. 145,* American Chemical Society, Washington, D. C., 1975.

Blanchard, D. C., Jet drop enrichment of bacteria, virus, and dissolved organic material, *Pure Appl. Geophys., 116,* 302–306, 1978.

Blanchard, D. C., and E. J. Hoffman, Control of jet drop dynamics by organic material in seawater, *J. Geophys. Res., 83,* 6187–6191, 1978.

Blanchard, D. C., and A. T. Spencer, Experiments on the generation of raindrop-size distributions by drop breakup, *J. Atmos. Sci., 27,* 101–108, 1970.

Blanchard, D. C., and L. Syzdek, Importance of bubble scavenging in the water-to-air transfer of organic material and bacteria, *J. Rech. Atmos., 8,* 529–540, 1974.

Blanchard, D. C., and L. Syzdek, Electrostatic collection of jet and film drops, *Limnol. Oceanogr., 20,* 762–774, 1975.

Blanchard, D. C., and A. H. Woodcock, Bubble formation and modification in the sea and its meteorological significance, *Tellus, 9,* 145–158, 1957.

Blanchard, D. C., and A. H. Woodcock, The production, concentration and vertical distribution of the sea-salt aerosol, *Ann. N.Y. Acad. Sci., 338,* 330–347, 1980.

Cipriano, R. J., Bubble and aerosol spectra produced by a laboratory simulation of a breaking wave, Ph.D. dissertation, State Univ. of New York, Albany, 1979.

Cokelet, E. D., Breaking waves, *Nature, 267,* 769–774, 1977.

Day, J. A., Small droplets from rupturing air-bubble films, *J. Rech. Atmos., 7,* 191–196, 1963.

Detwiler, A., and D. C. Blanchard, Aging and bursting bubbles in trace-contaminated water, *Chem. Eng. Sci., 33,* 9–13, 1978.

Iribarne, J. V., D. Corr, B. Y. H. Liu, and D. Y. H. Pui, On the hypothesis of particle fragmentation during evaporation, *Atmos. Environ. 11,* 639–642, 1977.

Johnson, B. D., and R. C. Cooke, Bubble populations and spectra in coastal waters: A photographic approach, *J. Geophys. Res., 84,* 3761–3766, 1979.

Kolovayev, P. A., Investigation of the concentration and statistical size dsitribution of wind-produced bubbles in the near-surface ocean layer, *Oceanol. Acad. Sci. USSR, 15,* 659–661, 1976.

Liu, B. Y. H., and D. Y. H. Pui, On the performance of the electrical aerosol analyser, *J. Aerosol Sci., 6,* 249–264, 1975.

Lovik, A., Acoustic measurements of the gas bubble spectrum in water, in *Cavitation and Inhomogeneities in Underwater Acoustics,* edited by W. Lauterborn, pp. 211–218, Springer-Verlag, Berlin, 1980.

Mason, B. J., The oceans as source of cloud-forming nuclei, *Geof. Pura Appl., 36,* 148–155, 1957.

Mason, B. J., *The Physics of Clouds,* pp. 77–79, Clarendon, New York, 1971.

Medwin, H., In situ acoustic measurements of microbubbles at sea, *J. Geophys. Res., 82,* 971–976, 1977.

Monahan, E. C., The influence of whitecaps on the marine atmosphere, annual report, Univ. Coll., Galway, Ireland, 1979.

Moore, D. J., and B. J. Mason, The concentration, size distribution and production rate of large salt nuclei over the oceans, *Q. J. R. Meteorol. Soc., 80,* 583–590.

Paterson, M. P., and K. T. Spillane, Surface films and the production of sea-salt aerosol, Q. J. R. *Meteorol. Soc., 95,* 526–534, 1969.

Sinclair, D., R. J. Countess, Y. H. Liu, and D. Y. H. Pui, Experimental verification of diffusion battery theory, *J. Air Pollut. Control Assoc., 26,* 661–663, 1976.

Srivastava, R. C., Parameterization of raindrop size distributions, *J. Atmos. Sci., 35,* 108–117, 1978.

Woodcock, A. H., Smaller salt particles in oceanic air and bubble behavior in the sea, *J. Geophys. Res., 77,* 5316–5321, 1972.

Wu, J., Bubble populations and spectra in near-surface ocean: Summary and review of field measurements, *J. Geophys. Res., 86,* 457–463, 1981.

(Received July 28, 1980;
revised April 6, 1981;
accepted April 24, 1981.)